

# Prediction and optimization of electrospinning parameters for polymethyl methacrylate nanofiber fabrication using response surface methodology and artificial neural networks

Hossein Mohammad Khanlou · Ali Sadollah ·  
Bee Chin Ang · Joong Hoon Kim · Sepehr Talebian ·  
Azadeh Ghadimi

Received: 12 November 2013 / Accepted: 17 January 2014 / Published online: 30 January 2014  
© Springer-Verlag London 2014

**Abstract** Since the fiber diameter determines the mechanical, electrical, and optical properties of electrospun nanofiber mats, the effect of material and process parameters on electrospun polymethyl methacrylate (PMMA) fiber diameter were studied. Accordingly, the prediction and optimization of input factors were performed using the response surface methodology (RSM) with the design of experiments technique and artificial neural networks (ANNs). A central composite design of RSM was employed to develop a mathematical model as well as to define the optimum condition. A three-layered feed-forward ANN model was designed and used for the prediction of the response factor, namely the PMMA fiber diameter (in nm). The parameters studied were polymer concentration (13–28 wt%), feed rate (1–5 mL/h), and tip-to-collector distance (10–23 cm). From the analysis of variance, the most significant factor that caused a remarkable impact on the experimental design response was identified. The predicted responses using the RSM and ANNs were compared in figures and tables. In general, the ANNs outperformed the RSM in terms of accuracy and prediction of obtained results.

**Keywords** Electrospinning parameters · Polymethyl methacrylate (PMMA) · Nanofibers · Response surface methodology · Artificial neural networks

## 1 Introduction

The current priority of global materials research is focused on exploring nanomaterials, due to the numerous likely applications of nanotechnology in areas such as biotechnology, defense, and even in the semiconductor industry [1, 2]. To date, a significant amount of research on nanoscale fibers has been performed to pursue potential application areas including tissue-engineered membranes [3], nano-resonators [4], micro-air vehicles [5], and hydrophobic thin films [6].

As a matter of fact, the electrospinning process, also known as electrostatic fiber spinning, has shown an impressive capability to consistently manufacture nanoscale fibers either from synthetic or natural polymers [7]. The resulting fiber normally determines the mechanical, electrical, and optical properties of electrospun fiber mats.

As previously shown, both the strength and conductivity of the film/mat of fibers manufactured using the electrospinning process are sensitive to fiber diameter [1]. Therefore, it has been concluded that it is vital to control the fiber diameter that is a function of material and process parameters.

Several studies have investigated the electrospinning process [1, 2, 8]. However, when it comes to the effects of the process and material parameters on fiber formation, both theoretical and experimental investigations are being continually conducted [9–11].

Polymethyl methacrylate (PMMA) is known to be a transparent thermoplastic polymer with an amorphous

---

H. M. Khanlou · B. C. Ang · S. Talebian  
Center of Advanced Materials, Department of Mechanical Engineering, University of Malaya, Kuala Lumpur 50603, Malaysia

A. Sadollah · J. H. Kim (✉)  
School of Civil, Environmental and Architectural Engineering, Korea University, Seoul 136-713, South Korea  
e-mail: jaykim@korea.ac.kr

A. Ghadimi  
Department of Mechanical Engineering, School of Engineering, Taylor's University, Kuala Lumpur, Malaysia

structure [12]. Given that fact, PMMA has been recognized to have important applications including use as a transparent glass substitute for eye lenses, implants, and artistic and esthetic articles.

In the past few years, numerous studies have concentrated on the manufacturing of PMMA and other polymers by means of the electrospinning process with a focus on the fiber diameter. All of them reported varying results on the effects of electrospinning parameters and polymer concentration on the fiber diameter. Most of them concluded that a large fiber diameter is the main problem with their results [13–15].

The design of experiments (DOE) method is an important tool for the planning optimization of experimental research. DOE plays an important role in estimating the effect of several variables, and whether these specific variable need to be evaluated separately, simultaneously or as a combination of the two [16].

The response surface methodology (RSM) is a statistical method intended for demonstrating and analyzing the existing relationships concerning several input and response variables [17]. The RSM is a practical modeling method which involves using polynomials in place of local approximations to the true input or output relationship. Using the RSM, the objective is to improve the optimized response (output variables) that is influenced by several independent variables (input variables).

This approach will benefit from using RSM to lessen the requirement for carrying out repeated experiments for tests with multiple factors [18]. Recently, Low et al. [19] in their recent study applied RSM to the optimization of the mechanical properties of composite materials.

Artificial neural networks (ANNs) are a mathematical or computational model that is constructed using inspiration from the structural and/or functional aspects of biological neural networks. This particular network consists of dense interconnected computing units (artificial neurons) characterized by simple mathematical models of complex neurons in biological systems.

During the learning (training) process, information is obtained and later stored in the synaptic weights of the inter-nodal connections. The use of ANNs provides the advantage of being able to represent complex input–output relationships and is ideal when used for performing data classification, function approximation, signal processing, and so forth. The concept for the majority of ANNs was defined by Hassoun [20], while Hertz et al. [21] formulated the mathematics for ANNs in a methodical manner. Sha and Edwards [22] comprehensively researched the application of ANNs in material science.

Hassan et al. [23] utilized ANNs to calculate density, porosity, and hardness of a based composite material. In addition, Xiao and Zhu [24] used the application of ANNs

and RSM to study the development of friction materials. Singh et al. [25] predicted the effective thermal conductivity of moist porous materials using ANNs. A review paper [26] confirmed that employing ANNs has significantly stimulated investigation in the field of material science and technology [27].

The purpose of this paper is to study the effects of the electrospinning parameters on the PMMA nanofiber diameter and to also find the optimum conditions for electrospinning PMMA nanofibers. The PMMA nanofibers in this study had a diameter under 200 nm, the smallest diameter among all previous studies on the fabrication of PMMA nanofibers [13, 14]. The RSM and ANNs have been employed to predict the optimal parameters for electrospinning. Statistical results and an optimization phase using the RSM accompanied by ANNs prediction were performed and compared.

The remainder of the paper is organized as follows. The next section describes the materials and methods used. Detailed explanations regarding the preparation of material and applied methods are given in Sect. 2. In Sect. 3, statistical and predicted results using the RSM and ANNs are provided, respectively. Also, a comparison of the RSM and ANNs in terms of error percentage and linear regression is given in Sect. 3. The optimization phase for the PMMA nanofiber is discussed in Sect. 4. The optimum condition and the desirability of the PMMA fiber diameter are obtained in Sect. 4. Finally, conclusions are drawn in Sect. 5.

## 2 Material and applied methods

### 2.1 Material and electrospinning process preparation

A mixture of analytically pure polymethyl methacrylate (PMMA,  $(-\text{CH}_2\text{C}(\text{CH}_3)\text{CO}_2\text{CH}_3)_n$ ,  $M_w = 120,000$ ), sourced from Aldrich, and N,N-dimethylformamide (DMF), sourced from Labchem Sdn Bhd Co., Malaysia, was used as the working solution in this study. Correspondingly, polymer solution samples were obtained by dissolving 13–28 wt% PMMA in the DMF solvent.

In addition, an ES30P-30W/SDPM (Gamma High Voltage Research, Ormond Beach, FL) unit was used as a good source for high-voltage power supply. Using a voltage of 15 kV, a suitable Taylor cone was produced and was intended to be used for all experiments. A connection between the high-voltage power supply and the needle was made using an alligator clip.

In addition, a counter electrode was created by means of a ground target at different tip-to-collector distances altering from 10 to 23 cm. The ground target was covered with aluminum foil. In addition, a syringe pump (NE-300,

New Era Pump Systems, Inc.) was used to regulate the feed rate at different rates from 1 to 5 mL/h.

The different processes employed for the fabrication of the PMMA nanofibers are as follows. (a) Drawing: a micropipette a few micrometers in diameter is dipped into the working solution near the contact line using a micro-manipulator. Subsequently, the micropipette is withdrawn from the liquid and moved at a certain speed resulting in a nanofiber being pulled; (b) template synthesis: template synthesis entails the use of a template or mold to obtain the desired material or structure. By applying water pressure and restraining using a porous membrane, the polymer nanofiber is extruded. The diameter of the nanofibers is determined by the pore size during solidification of the solution; (c) electrospinning: electrospinning is a process by which a charged liquid polymer solution is exposed to an electric field. The liquid polymer solution is dispensed via a needle attached to a syringe held at a certain voltage and is deposited on a conductive material, which is grounded (zero voltage), located at some distance from the needle.

The main advantages of the electrospinning process over the other two (drawing and template synthesis) methods are scalability, controllability, repeatability, and industrialization potential in the case of nozzleless electrospinning. Therefore, the electrospinning process was carried out at a temperature of 25 °C and 32 % relative humidity (RH) as it is vital to choose appropriate conditions of temperature and RH.

In order to obtain control over the nanofiber diameter, the polymer concentration, collector distance, and feed rate were modified. Finally, by using the Digimizer 4.1 software, the diameters of fifteen fibers were randomly measured from field-emission scanning electron microscope (FESEM) images.

Using the Digimizer software, the fiber diameter was measured at three different places for each of the fifteen fibers in the image. The measured image of the PMMA fibers is shown in Fig. 1 using the Digimizer software. Measured fiber diameters are highlighted in bright colors in Fig. 1.

The experimental set-up used for electrospinning and a typical FESEM image of an electrospun PMMA nanofiber mat are shown in Fig. 2.

## 2.2 Design of experiments

The influence of the electrospinning process parameters on the PMMA fiber diameter was investigated using the RSM. In this study, the three operating variables (feed rate, collector distance, and polymer concentration) were developed by applying central composite design and the RSM.

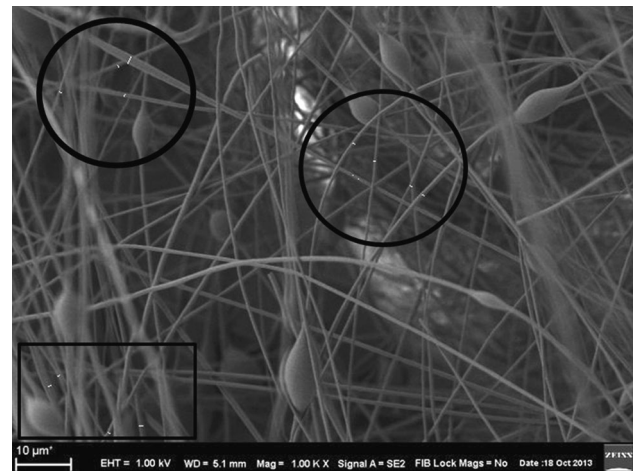


**Fig. 1** Measured image of the PMMA fibers diameter

The choice of tip-to-collector distance range is directly related to solvent evaporation and fiber formation. If this distance is less than 10 cm, the polymer solution does not have enough time to change into a fiber shape due to the presence of the high-voltage fields. On the other hand, if the tip-to-collector distance is too large (e.g., more than 20 cm), the created fibers cannot fly properly toward the collector. In other words, in a range of 10–20 cm, the polymer solution has enough traveling time (from needle to the collector). The suggested range for the distance ratio was based on the recommendation in the literature [15].

The polymer concentration has a major effect on the solution viscosity, which is a key factor in the electrospinning process. A low concentration would lead to low viscosity and defective fibers. A high concentration would result in defective fibers because of high viscosity. Therefore, based on the suggestions in literature, the suitable concentration range for obtaining an acceptable fiber diameter is determined based on a trial-and-error approach [14, 15].

Input feed rate plays an important role in determining the fiber diameter. **Since the purpose of this research is to control the PMMA nanofiber diameter,** the feed rate was optimized to obtain nanometer-range fiber diameters, and as a result, we were able to produce high-quality nanofibers [14, 15].

In this study, the fiber diameter (in nm) is considered as the response of the system, and the Design-Expert software (version 8.0) was used for the statistical design of experiments and data analysis. The obtained results are shown in Table 1 based on the experimental tests.

As a result of experiencing difficulty and complexity in the process of performing experimental tests, only 14 experiments were carried out. Moreover, with the purpose of measuring the reproducibility of the process parameters,

**Fig. 2** Electrospinning set-up and FESEM image for the electrospun PMMA nanofiber

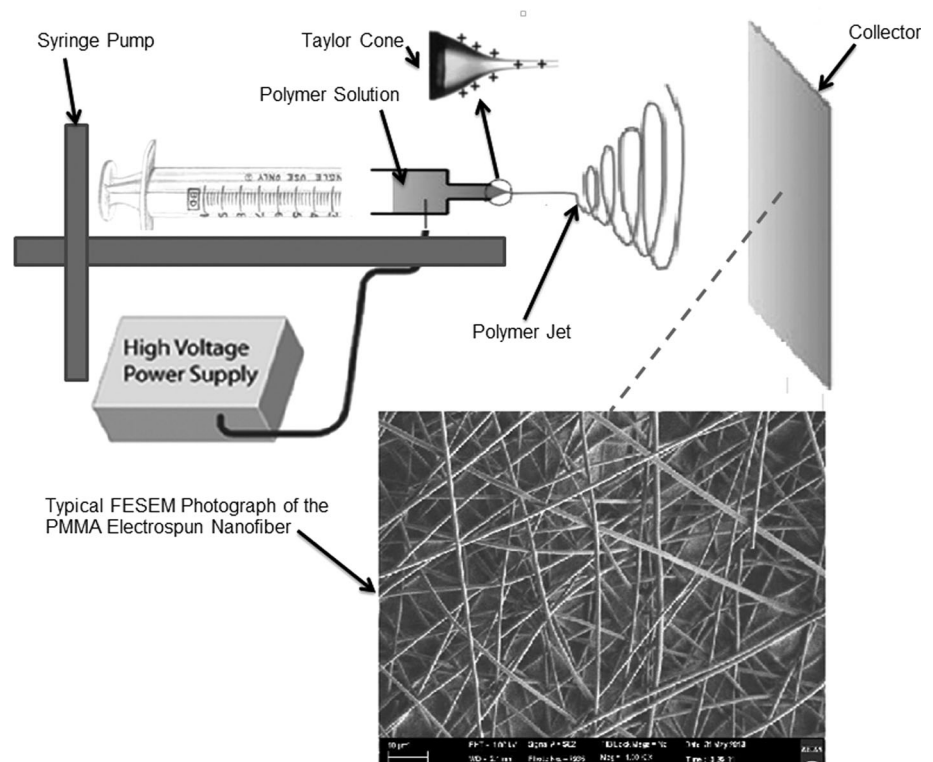


**Table 1** Experimental results obtained from 20 independent tests for the electrospun PMMA nanofibers

Run	Factor 1: polymer conc. (wt%)	Factor 2: feed rate (mL/h)	Factor 3: tip-to-collector distance (cm)	Response: fiber diameter (nm)
1	20	2.5	15	548
2	20	2.5	15	563
3	20	2.5	15	636
4	20	2.5	15	604
5	20	2.5	15	634
6	20	2.5	15	549
7	15	1	10	230
8	25	1	10	1,290
9	15	4	10	143
10	25	4	10	1,505
11	15	1	20	324
12	25	1	20	1,280
13	15	4	20	301
14	25	4	20	1,000
15	13	2.5	15	170
16	28	2.5	15	1,430
17	20	2	15	552
18	20	5	15	585
19	20	2.5	16	575
20	20	2.5	23	572

an additional 6 tests were carried out as center points of the experiment.

The number of center points increased the accuracy of the prediction and optimization results, as was proved in this work. In fact, six center points were suggested by the design-expert software upon choosing the central composite design, the best condition for achieving the desired results. Fiber diameter achieved as a response to varying the parameters was fitted in a quadratic model using regression analysis.

### 2.3 Artificial neural network implementation

#### 2.3.1 Introduction

The ANNs are a composition of simple elements functioning effectively in a parallel manner. These simple elements are derived from the concept of biological nervous systems. Logically, the network function is determined by identifying the connections between these elements. ANNs consist of numerous artificial neurons also known as processing units.

These processing units are arranged in a series of layers, namely input, hidden, and output layers. Multi-layer perceptron (MLP) is known to be the architecture of ANNs. The MLP networks consist of an input layer representing

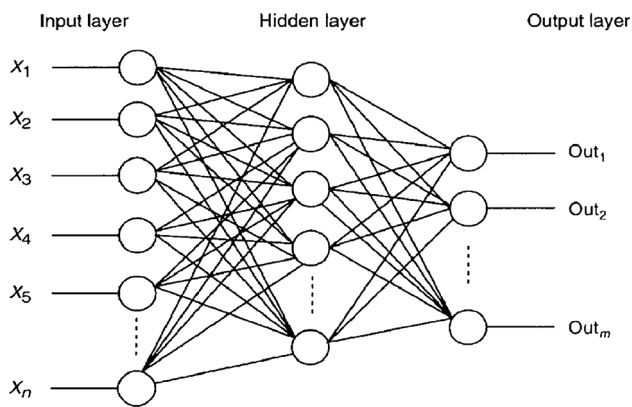


**Fig. 3** Schematic view of a typical multi-layer perceptron (MLP) network having three layers based on the back-propagation (BP) algorithm

the input parameters, an output layer representing the output parameters, and one or more hidden layers. In the past, a number of algorithms have been recommended for training ANNs, and the back-propagation (BP) algorithm [28] is found to be the most effective and studied learning algorithm. The BP algorithm is a simplification of the Widrow-Hoff learning rule and has been widely used for training MLP networks. It is based on the nonlinear differentiable transfer functions, which are normally sigmoid functions.

By using input vectors and the corresponding target (output) vectors, it is possible to train a network, so it can estimate a function to an arbitrary degree of accuracy. Represented in Fig. 3 is a typical architecture of a three-layered neural network. Furthermore, a number of resources on the fundamental theory and applications of BP-based ANNs are available [21, 29–32].

### 2.3.2 Input and output preparation

The input of the ANNs should be measured easily and accurately. In addition, it should be sensitive to the parameters of the electrospinning process. In this work, the polymer concentration, feed rate, and tip-to-collector distance parameters of electrospinning were chosen as the inputs of the ANNs. Consequently, the electrospun PMMA fiber diameter is chosen as the output of the ANNs.

An assumption about a nonlinear mapping existing between the stability and input parameters was made. Table 1 shows that only 20 tests were carried out owing to the difficulty in conducting experiments. With the purpose of training the ANNs, 65 % of the samples are randomly assigned to the training set. Then, 15 % of the samples are randomly assigned to the validation set.

In cases wherein the network performance on the validation vectors fails to improve, an early training termination is done by using validation vectors. Furthermore, in

conditions wherein the training error is noticeably reduced on the validation samples, a continuous training is performed. When the network simplifies the training set, the training is terminated.

By using this procedure, the problem of over-fitting during the training that can disrupt the optimization and learning algorithms was automatically prevented. Finally, an independent test of the trained ANNs simplification is provided by the remaining 20 % of the samples (unseen samples). Additionally, test vectors are used in order to check that the ANNs were being well-generalized. However, it does not have any effect on the training [33]. Normalizing the input and output data before training is also highly suggested so as to avoid possible training saturation [34, 35]. Also, training is frequently completed faster when values are normalized.

### 2.3.3 ANNs architecture

The characterization of the architecture or topological structure of an ANNs can be done by identifying the arrangement of the layers and neurons, the nodal connectivity, and the nodal transfer functions. Moreover, simulation of any mapping from an input to output can be done by using a multilayered feed-forward neural network with a back-propagation algorithm.

As corroborated by Hecht-Nielsen [36], a three-layered feed-forward neural network with a back-propagation algorithm can be trained to estimate any mapping from  $n$  dimensions to  $m$  dimensions to an arbitrary degree of accuracy. In this study, a fully connected ANNs was used. This ANNs had two hidden layers and one output layer, and the number of neurons in the input, output, first, and second hidden layers were 2, 1, 20, and 10, respectively. The increase in the number of neurons apparently increases the computation but also gives the advantage of solving complicated problems more efficiently [33]. On the subject of the effects of the number of hidden layers and the learning factor on the expectation accuracy of ANNs, the reader may refer to a previous work [37].

Overall, a neural network with a single hidden layer is proficient in approximating any nonlinear function to an arbitrary degree of accuracy. Then again, an improvement in the ANNs training/learning for highly complex functions can be done by increasing the number of layers [38] as the ANNs are also sensitive to the number of neurons in their hidden layers.

Under-fitting is often a result of having too few neurons while too many neurons can result to over-fitting, which can be defined as all training points having been well-fitted. Additionally, the fitting curve oscillates wildly among these points. As a result, the transfer functions in the feed-



**Table 2** ANOVA results for the electrospun PMMA fiber for regression model equation and coefficients of model terms

Source	SS	df	Mean square	F value	Prob. >F
Model	3,113,818.687	9	345,979.8541	38.12103	<0.0001
A	2743595.756	1	2,743,595.756	302.2971	<0.0001
B	7,665.118487	1	7,665.118487	0.844564	0.3797
C	16,228.38157	1	16,228.38157	1.788089	0.2108
A <sup>2</sup>	66,651.12861	1	66,651.12861	7.343808	0.0219
B <sup>2</sup>	8,999.296419	1	8,999.296419	0.991568	0.3428
C <sup>2</sup>	12,732.04622	1	12,732.04622	1.402853	0.2636
AB	253.125	1	253.125	0.02789	0.8707
AC	73,536.125	1	73,536.125	8.102416	0.0174
BC	23,220.125	1	23,220.125	2.558458	0.1408

forward back-propagation network is assumed to be a tan-sigmoid, log-sigmoid, and linear transfer function for the first hidden layer, the second hidden layer, and the output layer, respectively. This specific structure is useful for function approximation (or regression) problems [33] since multiple layers of neurons with nonlinear transfer functions can allow the network to learn nonlinear and linear relationships between input and output vectors.

### 2.3.4 ANNs training and simulation

Generally, the simplification property of ANNs enables the possibility of training a network using a representative set of **input/target** pairs and achieve good results without training the network for all possible input/output pairs.

A learning rule, also referred to as a training algorithm, is described as a method used for the modification of the weights and biases of a network. The objective of using a learning rule is to train the network to perform a particular task. It entails two broad categories, namely supervised learning and unsupervised learning [33].

In order to perform ANN simulation work, we used MATLAB and the prediction task was carried out on a Pentium V 2.53 GHz system with 4 GB RAM. Additionally, a feed-forward neural network model with a back-propagation algorithm was employed for the network training and simulation.

Among other training functions, the **Levenberg–Marquardt training function** is often the fastest back-propagation algorithm. Given the fact that it does require more memory than other algorithms, it is also highly recommended as a first-choice supervised algorithm [38].

In this study, the Levenberg–Marquardt algorithm was used to control the learning process until a reasonable mean square error (MSE) value was attained. On the other hand, during the learning process the weights between the connections were adjusted by using the enhanced back-propagation algorithm.

## 3 Results and discussions

### 3.1 Statistical results obtained by design of experiment

The evaluation of the experimental results was performed using multiple regression analysis. For that reason, the best experimental model selected for this purpose is a quadratic model. Additionally, the analysis of variance (ANOVA) method was utilized for the approximation of the effects of the main variables and their potential interactions. A Pentium V 2.53 GHz system with 4 GB RAM was used for applying the RSM to the electrospun PMMA fiber diameter. Table 2 shows the statistical results of the electrospun fiber diameter obtained using ANOVA.

As can be seen in Table 2, the sum of squares (SS) is the sum of the squared deviations, DF is the degree of freedom, and the mean square is calculated as SS divided by DF. Moreover, the *F* values and associated probability are the important outputs of the model.

The model's *F* value of 38.12103 and *Prob. >F* value of less than 0.05 show that there is only a 0.01 % chance that a “model *F* value” occurred due to noise. **It also gives a clear indication that the model is significant at a confidence interval (CI) of more than 95 % for electrospun PMMA nanofibers.** In contrast, values greater than 0.1 indicate that the model terms are not significant.

In order to reach the highest *R-Squared* (0.9716) and high insignificant *Prob. >F* value (0.8707), the factor *AB* was eliminated. The following quadratic model equations are given by the regression analysis. These equations are established using the coded and actual factors of the RSM as given below:

$$\begin{aligned}
 \text{PMMA fiber diameter} = & + 582.19 + 471.18 \times A - 29.52 \\
 & \times B + 43.14 \times C + 82.42 \times A^2 \\
 & + 35.10 \times B^2 + 43.01 \times C^2 \\
 & - 95.88 \times AC - 53.87 \times BC
 \end{aligned}
 \quad (1)$$

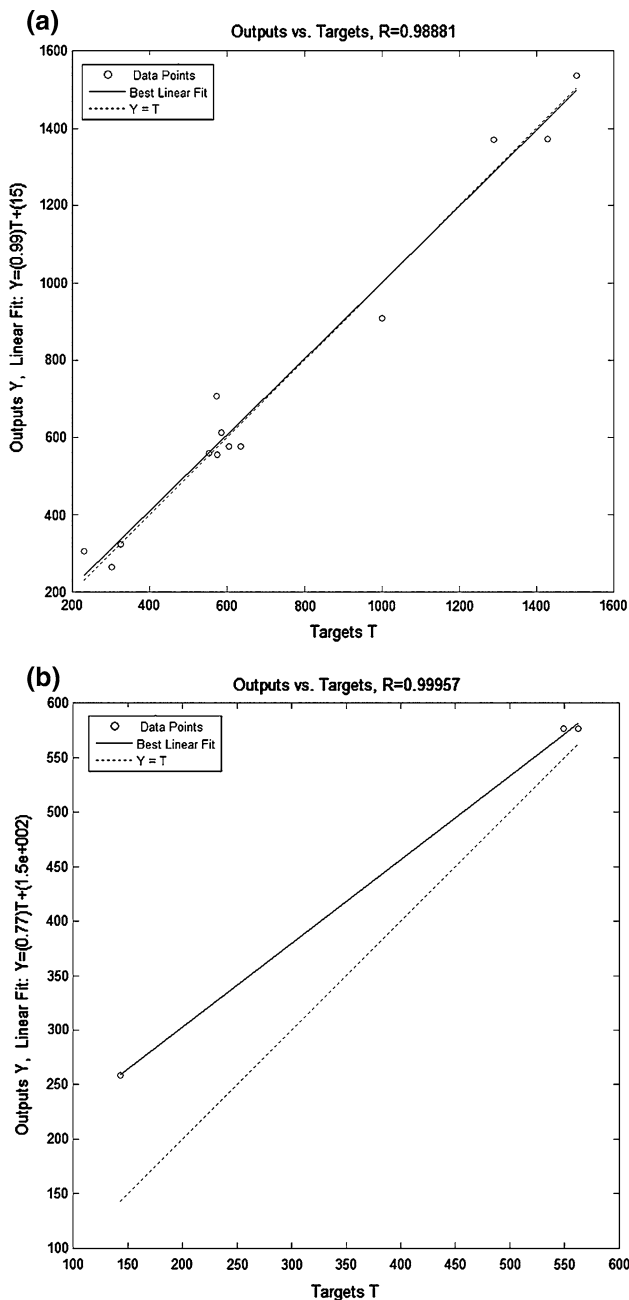


**Fig. 4** Correlation coefficient plot for the fiber diameter response of PMMA: **a** training samples, **b** validation samples

PMMA fiber diameter =

$$\begin{aligned}
 & -740.55372 + 19.89499 \times \text{Concentration} + 10.05867 \\
 & \times \text{Feed rate} + 34.42317 \times \text{Tip-to-collector distance} \\
 & + 3.29664 \times \text{Concentration}^2 + 15.60186 \times \text{Feed rate}^2 \\
 & + 1.72027 \times \text{Tip-to-collector distance}^2 - 3.83500 \\
 & \times \text{Concentration} \times \text{Tip-to-collector distance} - 7.18333 \\
 & \times \text{Feed rate} \times \text{Tip-to-collector distance} \quad (2)
 \end{aligned}$$

where  $A$ ,  $B$ , and  $C$  are coded factors representing the polymer concentration, feed rate, and tip-to-collector

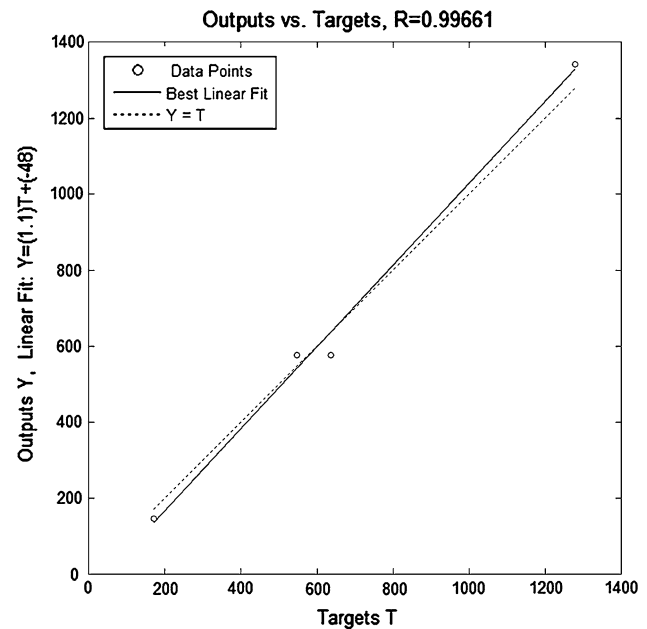


**Fig. 5** Correlation coefficient plot for test samples of the PMMA nanofiber diameter response (*vertical and horizontal axes are the predicted output and corresponding targets, respectively*)

distance, respectively. As shown in Table 2, the following ANOVA results clearly indicate that among the given parameters, **the terms  $A$ ,  $A^2$  and  $AC$  have shown a significant effect on the electrospun PMMA fiber diameter.**

Therefore, any change in the value of  $A$  (coded factor for polymer concentration) is expected to create a significant change in the value of the electrospun PMMA fiber diameter. Evidently, in comparison with the tip-to-collector distance and feed-rate factors, the PMMA fiber diameter is more reliant on the PMMA concentration.

### 3.2 Predicted results using ANNs

In this paper, a progressive ANNs procedure is applied to characterize the material properties of electrospun PMMA using nanofiber diameter as a response function. Twenty randomly selected experimental data points were used, categorized as thirteen data points for training, three data points for validation, and four unseen data points for testing the trained ANNs.

The fiber diameter is considered as a response (output) of the ANNs. Accordingly, the inputs of the ANNs are the polymer concentration, feed rate, and tip-to-collector distance factors. Figure 4 shows the correlation coefficient for the training and validation samples. It is a measure of how well the variation in the output is explained by the targets. If the correlation coefficient is equal to one, then there is a perfect correlation between targets and outputs. From Fig. 4a and b, the correlation factor for the training and

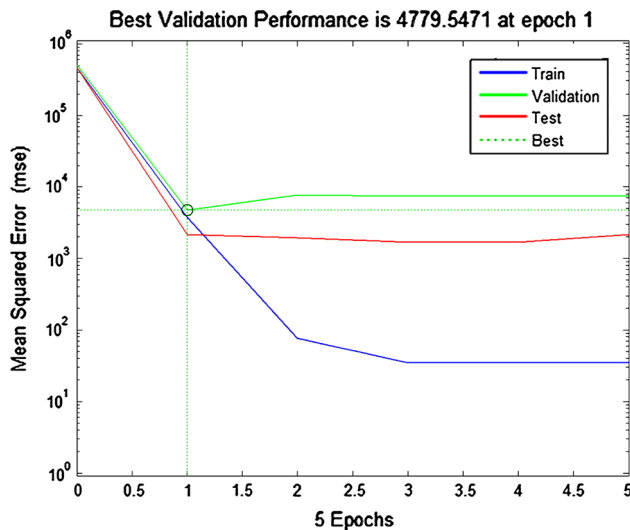


**Fig. 6** Mean square error (MSE) plot with respect to the number of epochs for training, validation, and test samples for the PMMA fiber diameter response

validation samples are 0.98 and 0.99, respectively, which indicates a good fit.

In order to make sure that the trained ANNs works properly, test samples must be applied, and afterward, the linear regression should again be measured. Four sample data were chosen randomly by ANNs to validate the performance of the trained ANNs. Figure 5 illustrates the linear regression of four sample data for the testing phase of the trained ANNs.

As can be seen, the correlation coefficient is 0.99 which demonstrates a good fit between the inputs and outputs for the unseen data. As mentioned in Sect. 2.3.4, the typical performance function that is used for training a feed-forward ANNs is the MSE for the network errors. This performance function causes the network to have smaller weights and biases. Also, the MSE forces the network response to be smoother and less likely to over fit.

The MSE plot for all samples including of training, validation, and test-sample errors are depicted in Fig. 6. The MSE of the network was started at a large value and decreased to a smaller value as shown in Fig. 6. In other words, Fig. 6 shows that the network is learning.

The training stopped when the validation error increased for five iterations, which occurred at epoch 1. In this case, the obtained results are reasonable because of the following considerations: the final MSE is small enough; the validation and test-set errors have similar characteristics; and no significant over-fitting has occurred by epoch 1 (where the best validation performance occurs). It is worth mentioning that if the MSE was too small, it meant that the ANNs memorized all the training data points instead of learning.

### 3.3 Comparison of RSM and ANNs

The obtained statistical results from the ANNs and RSM were compared in terms of error percentage and linear regression between the network outputs and the corresponding experimental results. Table 3 shows the comparison of experimental and predicted results for the fiber-diameter response obtained using RSM and ANNs. Four unseen test samples and their corresponding experimental data were compared as shown in Table 3.

The results obtained using the ANNs surpassed those attained using the RSM in three out of four cases, the former having a lower error percentage with respect to the experimental results (see Table 3). The lower error percentages have been highlighted in bold in Table 3 for each dataset.

The performance of an ANN can be measured to some extent by the errors in the training, validation, and test sets; however, it is often useful to investigate the network responses in more detail. One option is to perform a regression analysis between the network responses and the corresponding targets.

Figure 7 represents the linear regression between the predicted and actual experimental results for the PMMA nanofiber diameter response as open circles using the RSM and ANNs. The best linear fit is indicated by a dashed line.

A perfect fit (outputs equal to targets) is indicated by the solid line.  $m$  and  $b$  are the slope and the y-intercept, respectively, of the best linear regression fit relating the targets to the network outputs. If there was a perfect fit (outputs exactly equal to targets), the slope would be one and the y-intercept would be zero.

The correlation coefficient ( $R$  value) between the outputs and targets for the fiber diameter response are 0.99019 and 0.99661 for the RSM and ANNs, respectively, as depicted in Fig. 7. The values of  $m$  and  $b$  for RSM are 0.94 and  $-19.39$ , respectively.

Accordingly, the values of  $m$  and  $b$  for the ANNs are 1.075 and  $-48.47$ , respectively. As can be seen from the results compared in Table 3 and Fig. 7, the trained ANNs are superior to the RSM having a smaller error percentage and a high correlation coefficient factor ( $R$  value) for the PMMA fiber diameter response.

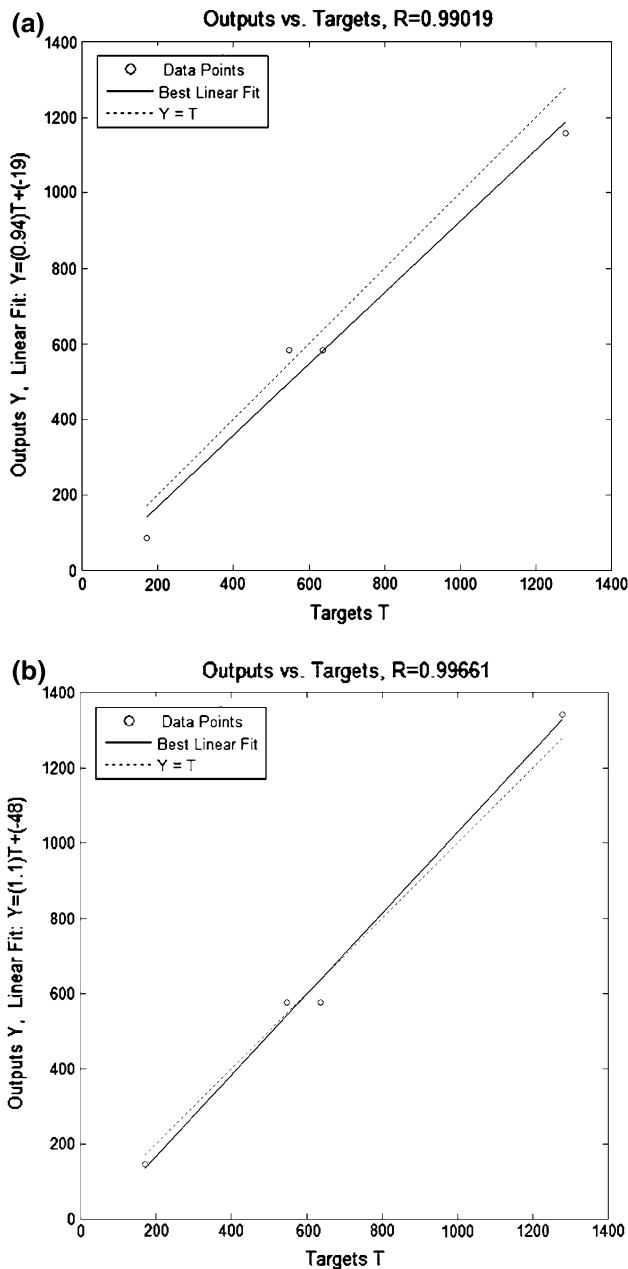
### 4 Parameter optimization of electrospun PMMA

The objective of this section is to optimize the electrospinning parameters (polymer concentration, feed rate, and tip-to-collector distance) for PMMA nanofibers. From the optimization point of view, it is important to attain the minimum values of the parameters for a given PMMA fiber diameter. In addition, since desirability involves multiple



**Table 3** Comparison of experimental and predicted results for the fiber diameter response obtained by the RSM and ANNs

Data	Polymer conc. (wt%)	Feed rate (mL/h)	Tip-to-collector distance (cm)	RSM (error %)	ANNs (error %)	Experimental (nm)
1	20	2.5	15	582.19 (+6.23)	576.72 (+5.24)	548
2	20	2.5	15	582.19 (−8.46)	576.72 (−9.32)	636
3	25	1	20	1,158.28 (−9.50)	1,341.31 (+4.78)	1,280
4	13	2.5	15	84.07 (−50.54)	145.20 (−14.58)	170

**Fig. 7** Parity plot among actual experiments and predicted values for the fiber diameter response obtained using the: **a** RSM, and **b** ANNs (vertical and horizontal axes are predicted output and corresponding targets, respectively)**Table 4** Optimum values and desirability for ten predicted points

No.	Polymer conc. (wt%)	Feed rate (mL/h)	Tip-to-collector distance (cm)	Fiber diameter (nm)	Desirability
1	<b>15.00</b>	<b>2.36</b>	<b>11.64</b>	<b>177.092</b>	<b>0.975</b>
2	15.00	2.34	11.63	177.097	0.975
3	15.00	2.14	11.27	177.472	0.975
4	15.00	2.07	10.83	177.821	0.974
5	15.00	2.04	10.99	177.881	0.974
6	15.00	2.85	12.95	179.217	0.973
7	15.00	1.34	10.00	185.92	0.968
8	15.00	3.53	14.85	189.278	0.966
9	15.00	3.50	12.37	192.525	0.964
10	15.00	2.90	20.00	269.261	0.907

responses from numerical optimization, the final response should discover a point that maximizes the desirability function.

The aim of the optimization is to find a good set of conditions that will meet all the goals, and not to get to a desirability value of one. The optimum desirability results (minimization) are tabulated in Table 4 for ten optimized prediction points. The best optimum condition is highlighted in bold.

Interestingly, in agreement with other studies [13, 39, 40] that were focused on the effect of polymer concentration on the formation of electrospun PMMA nanofibers, the optimum values for the electrospun PMMA nanofiber diameter were found to be highly dependent on the PMMA concentration. It should be noted that all ten optimized conditions suggested the fabrication of fibers using a 15 wt% PMMA concentration.

Noticeably, in the most optimized conditions, there are recommendations for a feed-rate factor altering around 2 mL/h, while the value of tip-to-collector distance was modified from a minimum of 10 cm to a maximum of 20 cm. By observing Table 4, the most desirable condition is selected using values of 15, 2.36, and 11.64 for the polymer concentration, feed rate and tip-to-collector distance factors, respectively.

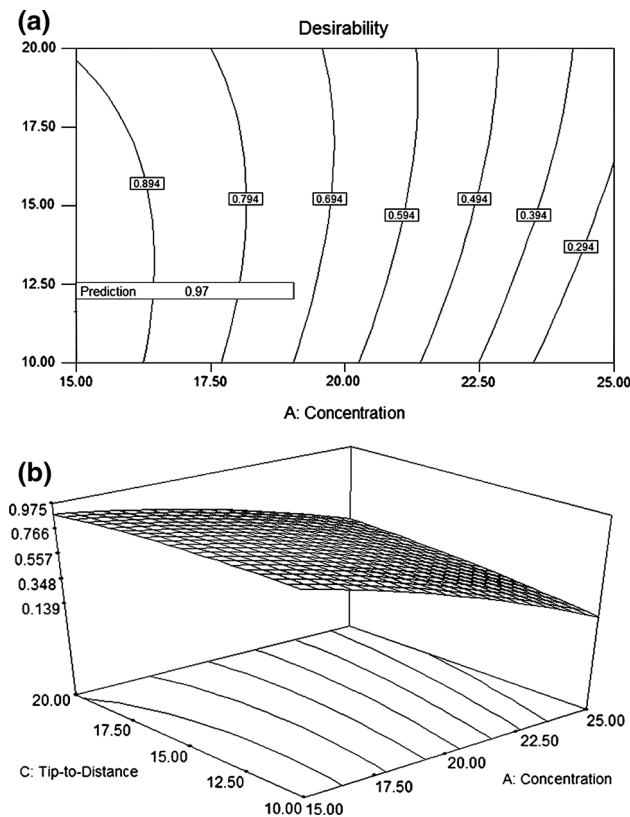


**Fig. 8** Desirability plot for the obtained mathematical model in: **a** 2D view, and **b** 3D view

Furthermore, this particular condition (highlighted in bold in Table 4) has a minimum fiber diameter value of 177.092 nm in comparison with other conditions. Also, the optimum condition possesses the best optimum value for desirability which is 0.975. Note that it is important to mention that the other predicted points have offered good suggestions. Figure 8 shows the obtained model for desirability plotted in 2D and 3D views for an optimum feed rate of 2.36 mL/h.

## 5 Conclusions

In this paper, the application of the response surface methodology (RSM) and ANNs was investigated in order to optimize and predict the electrospun PMMA fiber diameter (in nm). The inputs/factors were the polymer concentration (13–28 wt%), feed rate (1–5 mL/h), and tip-to-collector distance (15–23 cm). The current research was conducted to obtain a better understanding of the factors that have the greatest effect on the PMMA nanofiber diameter, thereby proposing a mathematical formulation using the RSM. The RSM showed that the PMMA concentration had a significant influence on the electrospun

fiber diameter. The optimum nanofiber diameter was obtained using values of 15, 2.36, and 11.64 for the polymer concentration, feed rate, and tip-to-collector distance, respectively. The results obtained from the RSM and ANNs were compared and discussed in figures and tables. In terms of the value of linear regression for the fiber diameter response, the results of the RSM and ANNs were close, with the ANNs slightly outperforming the RSM. Furthermore, the ANNs surpassed the RSM in terms of error percentage corresponding to the actual experimental results. The predicted effect of the each parameter on the formation of the nanofiber can be useful for fabricating other types of nanofibers. However, it should be noted that the effects of electrospinning parameters are highly dependent on the type of the polymer used.

**Acknowledgments** This work was supported by a National Research Foundation of Korea (NRF) grant funded by the Korean government (MSIP) (No. 2013R1A2A1A01013886) and the University of Malaya, grant No. RP022C-13AET.

## References

- Huang Z-M, Zhang YZ, Kotaki M, Ramakrishna S (2003) A review on polymer nanofibers by electrospinning and their applications in nanocomposites. *Compos Sci Technol* 63(15): 2223–2253
- Persano L, Camposeo A, Tekmen C, Pisignano D (2013) Industrial upscaling of electrospinning and applications of polymer nanofibers: a review. *Macromol Mater Eng* 298(5):504–520
- Jia L, Prabhakaran MP, Qin X, Kai D, Ramakrishna S (2013) Biocompatibility evaluation of protein-incorporated electrospun polyurethane-based scaffolds with smooth muscle cells for vascular tissue engineering. *J Mater Sci* 48(15):5113–5124
- Kameoka J, Verbridge SS, Liu H, Czaplewski DA, Craighead H (2004) Fabrication of suspended silica glass nanofibers from polymeric materials using a scanned electrospinning source. *Nano Lett* 4(11):2105–2108
- Pawlowski K, Belvin H, Raney D, Su J, Harrison J, Siochi E (2003) Electrospinning of a micro-air vehicle wing skin. *Polymer* 44(4):1309–1314
- Ma M, Hill RM (2006) Superhydrophobic surfaces. *Curr Opin Colloid Interface Sci* 11(4):193–202
- Reneker DH, Chun I (1996) Nanometre diameter fibres of polymer, produced by electrospinning. *Nanotechnology* 7(3):216
- Agarwal S, Greiner A, Wendorff JH (2013) Functional materials by electrospinning of polymers. *Prog Polym Sci* 38(6):963–991
- Hohman MM, Shin M, Rutledge G, Brenner MP (2001) Electrospinning and electrically forced jets. I. Stability theory. *Phys Fluids* 13:2201
- Reneker DH, Yarin AL (2008) Electrospinning jets and polymer nanofibers. *Polymer* 49(10):2387–2425
- Thompson C, Chase G, Yarin A, Reneker D (2007) Effects of parameters on nanofiber diameter determined from electrospinning model. *Polymer* 48(23):6913–6922
- Tanio N, Koike Y (2000) What is the most transparent polymer? *Fiber Optics Wkly Update*
- Piperno S, Lozzi L, Rastelli R, Passacantando M, Santucci S (2006) PMMA nanofibers production by electrospinning. *Appl Surf Sci* 252(15):5583–5586

14. Qian Y, Su Y, Li X, Wang H, He C (2010) Electrospinning of polymethyl methacrylate nanofibres in different solvents. *Iran Polym J* 19(2):123
15. Wang H, Liu Q, Yang Q, Li Y, Wang W, Sun L, Zhang C, Li Y (2010) Electrospun poly (methyl methacrylate) nanofibers and microparticles. *J Mater Sci* 45(4):1032–1038
16. Sánchez N, Martínez M, Aracil J (1997) Selective esterification of glycerine to 1-glycerol monooleate. 2. Optimization studies. *Ind Eng Chem Res* 36(5):1529–1534
17. Box GE, Draper NR (1987) Empirical model-building and response surfaces. Wiley, New Jersey
18. Indira V, Anjana R, George KE (2011) Preparation and characterization of PP/HDPE/NANOCLAY/SHORT fiber hybrid composites using response surface methodology. *Global J of Engg Appl Sci* 1(4):88–91
19. Low KL, Tan SH, Zein SHS, McPhail DS, Boccaccini AR (2011) Optimization of the mechanical properties of calcium phosphate/multi-walled carbon nanotubes/bovine serum albumin composites using response surface methodology. *Mater Des* 32(6):3312–3319
20. Hassoun MH (1995) Fundamentals of artificial neural networks. MIT press, Cambridge
21. Aleksander I, Morton H (1990) An introduction to neural computing, vol 240. Chapman and Hall, London
22. Sha W, Edwards K (2007) The use of artificial neural networks in materials science based research. *Mater Des* 28(6):1747–1752
23. Hassan AM, Alrashdan A, Hayajneh MT, Mayyas AT (2009) Prediction of density, porosity and hardness in aluminum–copper-based composite materials using artificial neural network. *J Mater Process Tech* 209(2):894–899
24. Xiao G, Zhu Z (2010) Friction materials development by using DOE/RSM and artificial neural network. *Tribol Int* 43(1):218–227
25. Singh R, Bhoopal R, Kumar S (2011) Prediction of effective thermal conductivity of moist porous materials using artificial neural network approach. *Build Environ* 46(12):2603–2608
26. Sumpter BG, Noid DW (1996) On the design, analysis, and characterization of materials using computational neural networks. *Annu Rev Mater Sci* 26(1):223–277
27. Giri Dev VR, Venugopal JR, Senthilkumar M, Gupta D, Ramakrishna S (2009) Prediction of water retention capacity of hydrolysed electrospun polyacrylonitrile fibers using statistical model and artificial neural network. *J Appl Polym Sci* 113(5):3397–3404
28. Li Y, Bridgwater J (2000) Prediction of extrusion pressure using an artificial neural network. *Powder Technol* 108(1):65–73
29. Hinton GE (1992) How neural networks learn from experience. *Sci Am* 267(3):145–151
30. Widrow B, Lehr MA (1993) Adaptive neural networks and their applications. *Int J Intell Syst* 8(4):453–507
31. Hecht-Nielsen R (1989) Theory of the backpropagation neural network. *Neural Netw IEEE IJCNN* 1:593–605
32. Basheer I, Hajmeer M (2000) Artificial neural networks: fundamentals, computing, design, and application. *J Microbiol Meth* 43(1):3–31
33. Demuth H, Beale M (2000) Neural network toolbox user's guide. The MathWorks, Inc, Natick
34. Adeli H (2001) Neural networks in civil engineering: 1989–2000. *Comput-Aided Civ Inf* 16(2):126–142
35. Yu J, Wu B (2009) The inverse of material properties of functionally graded pipes using the dispersion of guided waves and an artificial neural network. *NDT and E Int* 42(5):452–458
36. Hecht-Nielsen R (1988) Neurocomputer applications. *Neural Comput* 41:445–453
37. Lee T, Jeng DS (2002) Application of artificial neural networks in tide-forecasting. *Ocean Eng* 29(9):1003–1022
38. Hagan MT, Demuth HB, Beale MH (1996) Neural network design. Pws Pub, Boston
39. Gupta P, Elkins C, Long TE, Wilkes GL (2005) Electrospinning of linear homopolymers of poly (methyl methacrylate): exploring relationships between fiber formation, viscosity, molecular weight and concentration in a good solvent. *Polymer* 46(13):4799–4810
40. Macossay J, Marruffo A, Rincon R, Eubanks T, Kuang A (2007) Effect of needle diameter on nanofiber diameter and thermal properties of electrospun poly (methyl methacrylate). *Polym Adv Technol* 18(3):180–183